

COUPLED CONVECTIVE HEAT TRANSFER FROM AN INCLINED FLAT PLATE ENCLOSURE

H. M. Badr* and M. S. Siddiqui

*Department of Mechanical Engineering
King Fahd University of Petroleum & Minerals
Dhahran, Saudi Arabia*

الخلاصة :

يُعنى هذا البحث بدراسة تأثير التقارن بين انتقال الحرارة بالحمل الطبيعي داخل نطاق مستطيل ، وانتقال الحرارة بالحمل القسري خارج هذا النطاق . ويتميز السطح السفلي للنطاق بدرجة حرارة ثابتة بينما تكون جدرانه الجانبية معزولة حراريا . ويميل النطاق بزواوية تتراوح بين (٤٠° ، ٩٠°) كما تتراوح نسبة طول النطاق إلى عرضه ما بين (١ إلى ١٠) . وقد تمت الدراسة لرقم رايلي (Rayleigh number) حتى (٨٠٠٠) بينما يتغير رقم رينولد (Reynolds number) حتى (٣٠٠٠٠٠) . ولقد أُجريت العمليات الحسابية لمشكلة نمطية (حمل طبيعي داخلي فقط) بهدف مقارنة النتائج بالأبحاث المنشورة وذلك لاختبار دقة الطريقة العددية المستخدمة في الحل . وقد أظهرت الدراسة أن تأثير التقارن مع الحمل القسري الخارجي هو انخفاض معدل انتقال الحرارة بالمقارنة بالمشكلة النمطية . وقد حدث أعلى معدل لانتقال الحرارة عندما كانت نسبة الطول إلى العرض (٢) كما قل مع ازدياد هذه النسبة . كما أدى ازدياد زاوية الميل إلى تناقص معدل انتقال الحرارة عندما كانت نسبة الطول إلى العرض أقل من (٤) بينما أدى إلى ازدياد هذا المعدل عندما كانت نسبة الطول إلى العرض أكبر من (٤) . وقد حدثت ظاهرة انعكاس درجة الحرارة في النطاق وتأثرت هذه الظاهرة قليلا بظروف الانسياب الخارجي . كما أظهرت النتائج أيضا أن الانسياب الأحادي الاتجاه يؤدي إلى إنخفاض معدل انتقال الحرارة بالمقارنة بالانسياب ذي الاتجاه المتعاكس .

*Address for correspondence:
KFUPM Box No. 322
King Fahd University of Petroleum & Minerals
Dhahran 31261
Saudi Arabia

ABSTRACT

The problem of the coupling effect between free convection inside a rectangular enclosure and forced convection outside is investigated. The bottom plate of the enclosure is isothermal while the two side walls are adiabatic. The enclosure which is inclined at angles between 40° and 90° has an aspect ratio AR ranging from 1 to 10. The Rayleigh number (based on the height of the enclosure) is in the range $Ra < 8 \times 10^3$ while the Reynolds number of the external flow $Re < 3 \times 10^5$. The accuracy of the numerical scheme used for solving the governing equations is first verified by solving the standard cavity problem (internal free convection only) and comparing results with those obtained by previous investigators. The coupling effect between the internal and external regimes resulted in a reduction in the heat rate in comparison with the standard problem. The rate of heat transfer is found to be maximum at $AR = 2$ and decreases with further increase of AR . The increase of the inclination angle is found to reduce the heat transfer for $AR < 4$ while increasing it for $AR > 4$. The temperature reversals occur inside the enclosure and are slightly affected by the external flow. The unidirectional flow results in heat transfer rates lower than those obtained for the corresponding counterflow regime.

COUPLED CONVECTIVE HEAT TRANSFER FROM AN INCLINED FLAT PLATE ENCLOSURE

NOTATION

a_0, a_1, a_2	Coefficients in Equation (14)
AR	Aspect ratio: $AR = L/H$
C_p	Specific heat at constant pressure
g	Acceleration due to gravity
Gr	Grashof number: $Gr = g \beta H^3 (T_H - T_x) / \nu^2$
h, \bar{h}	Local and average heat transfer coefficients
H	Height of the cavity
I	Variational functional
k	Thermal conductivity
L	Length of the cavity
Nu, \bar{Nu}	Local and average Nusselt numbers
Pr	Prandtl number: $Pr = \mu C_p / k$
q_0	Flux
Ra	Rayleigh number: $Ra = \rho g \beta H^3 (T_H - T_x) / \mu \alpha$
Re	Reynold's number: $Re = \rho U L / \mu$
T	Temperature
u, v	Dimensionless velocities in the x and y directions
U	Free stream velocity
x, y	Dimensionless coordinates

Greek Symbols

α	Thermal diffusivity
β	Coefficient of thermal expansion
∇^2	The Laplacian operator: $\nabla^2 = \partial^2 / \partial x^2 + \partial^2 / \partial y^2$
ζ	Dimensionless vorticity
θ	Angle of inclination
μ	Absolute viscosity
ν	Kinematic viscosity
ρ	Fluid density
ϕ	Dimensionless temperature: $\phi = (T - T_x) / (T_H - T_x)$
ψ	Dimensionless stream function

Subscripts

H	Hot plate
w	Wall
∞	Far away from the enclosure

1. INTRODUCTION

The phenomenon of confined natural convection has been a source of challenge to theoreticians and

experimentalists for several decades. Buoyancy driven flows in confined spaces occur in many practical applications such as thermal insulation of buildings, cooling fluids in channels surrounding the core of nuclear reactors, cooling of electronic equipment, and underground electric cables. Recently, there has been more interest towards the improvement of the efficiency of flat plate solar collectors by reducing the heat loss through the cover plates. An extensive literature survey of such work has been given by Catton [1] and Karayiannis [2]. The bulk of this research was devoted to studying the convection phenomenon within cavities in vertical, inclined, or horizontal positions. Based on these studies, the heat losses were calculated assuming isothermal upper and lower surfaces. Although this assumption led to great simplification of the problem it does not take into consideration the thermal interaction between the internal free convection and the external heat transfer regime.

The first study on the thermal interaction between internal and external convection for a vertical square cavity was carried out by Sparrow and Prakash [3]. In their study, the hot plate was isothermal while the cold plate was subjected to an external natural convection boundary-layer flow. The range of Grashof number considered is $10^3 < Gr < 10^7$ while the Prandtl number $Pr = 0.7$. The interaction between the two regimes resulted in about a 40% reduction in the heat transfer rate. Recent studies of coupled convection from a rectangular cavity were carried out by Saidi [4], and Saidi, Tarasuk, and Base [5]. The first one [4] represents an experimental investigation of the coupling effect for a horizontal cavity with an aspect ratio in the range $8.85 < AR < 36.8$ and Rayleigh number in the range $10^3 < Ra < 10^5$. The effect of an external forced convection on the top plate was found to moderately affect the free convection regime within the cavity.

The problem of the coupled convective heat transfer from an inclined solar collector was investigated experimentally by Karayiannis and Tarasuk [6]. External natural convection was assumed on the top surface of a rectangular enclosure. The study considered the ranges $Ra < 6 \times 10^5$, $6.68 < AR < 33.4$, and angles of inclination between 15° and 60° . The temperature on the cold plate was found to increase monotonically with distance from the leading edge.

Temperature reversals also occurred and became more pronounced with increasing angle of inclination. The heat rates for the coupled convection at high Rayleigh numbers were found to be lower than those obtained for the case of isothermal cold plate. Detailed experimental results were also reported in [2] for the effect of coupling between the internal free convection and external forced convection.

To the best of the authors' knowledge, no other work has been reported dealing with this phenomenon. This work aims to investigate theoretically the coupling effect between an internal laminar free convection and an external forced convection for an inclined flat plate enclosure. A solution scheme that incorporates thermal interactions between the internal and external flows has been developed. The effect of aspect ratio, angle of inclination, Rayleigh number, and Reynolds number on the heat transfer are investigated. Numerical solutions were carried out for enclosures with aspect ratios ranging from 1 to 10 and inclined at angles between 40° and 90° . The Rayleigh number ranged between 2×10^3 and 8×10^3

while the external flow Reynolds number was either 6×10^4 or 3×10^5 . The problem is investigated when the flows on the top (forced) and bottom (natural) of the cold plate are either in the same direction (unidirectional flow) or in opposite directions (counter flow).

2. PROBLEM STATEMENT AND GOVERNING EQUATIONS

In this problem, a rectangular enclosure ABCD of width L and height H is inclined at an angle θ with the horizontal, as shown in Figure 1. The lower plate (AB) is hot and has a uniform temperature distribution while the two side walls (BC and AD) are thermally insulated. The top plate (CD) is cold and subjected to an external forced convection regime on the upper side. The flow inside the enclosure is steady and driven by buoyancy forces. The flow is considered incompressible and viscous heat dissipation is neglected. By invoking the Boussinesq approximation, the equations governing the flow and heat transfer can be expressed in a dimensionless form as:

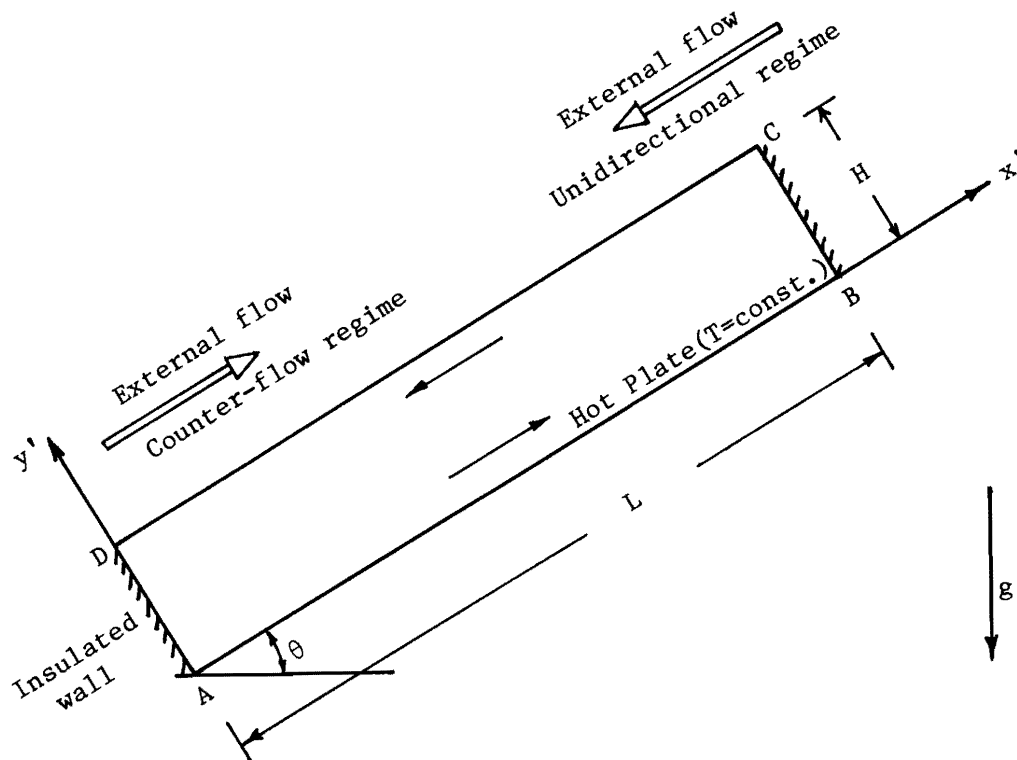


Figure 1. Schematic Representation of the Enclosure Showing the Direction of the External Flow for Unidirectional and Counter Flow Regimes.

$$\frac{1}{Pr} \left(\frac{\partial \psi}{\partial y} \frac{\partial \zeta}{\partial x} - \frac{\partial \psi}{\partial x} \frac{\partial \zeta}{\partial y} \right) - Ra \left(\frac{\partial \phi}{\partial x} \cos \theta - \frac{\partial \phi}{\partial y} \sin \theta \right) = \nabla^2 \zeta \quad (1)$$

$$\zeta = -\nabla^2 \psi \quad (2)$$

$$\frac{\partial \psi}{\partial y} \frac{\partial \phi}{\partial x} - \frac{\partial \psi}{\partial x} \frac{\partial \phi}{\partial y} = \nabla^2 \phi, \quad (3)$$

where $Pr = \mu C_p/k$ is the Prandtl number, $Ra = g \beta H^3 (T_H - T_\infty)/\nu \alpha$ is the Rayleigh number and the velocity components u and v are related to the stream function ψ by

$$u = \frac{\partial \psi}{\partial y}, \quad v = -\frac{\partial \psi}{\partial x} \quad (4)$$

The dimensionless variables ($x, y, \psi, u, v, \zeta, \phi$) used in Equation (1-4) are normalized using:

$$x = \frac{x'}{H}, \quad y = \frac{y'}{H}, \quad \psi = \frac{\psi'}{\alpha}, \quad \zeta = \frac{\zeta' \alpha}{L}$$

$$\phi = \frac{T - T_\infty}{T_H - T_\infty}, \quad u = \frac{u' H}{\alpha}, \quad v = \frac{v' H}{\alpha},$$

where all quantities with primes are dimensional.

In addition to the thermal boundary conditions explained above, the velocity field is characterized by the no-slip and impermeability conditions at the four solid walls of the enclosure. The boundary conditions can then be expressed as,

$$u = v = \psi = 0, \quad \phi = 1 \quad \text{at } y = 0 \quad (5a)$$

$$u = v = \psi = 0, \quad \phi = \phi(x) \quad \text{at } y = 1 \quad (5b)$$

$$u = v = \psi = 0, \quad \frac{\partial \phi}{\partial x} = 0 \quad \text{at } x = 0 \text{ and } x = AR, \quad (5c)$$

where $AR = L/H$ is the aspect ratio. The function $\phi(x)$ in Equation (5b) describes the temperature distribution on the top plate (CD) and is to be determined from the solution. The forced flow approaching the upper side of CD is assumed to have a uniform temperature T_∞ which will be referred to as the ambient temperature.

3. THE METHOD OF SOLUTION

The method used for solving the present problem deals with two different heat transfer regimes having the top plate (CD) as a common boundary. The conservation equations and boundary conditions

governing the flow inside the enclosure are different from those to be used for the external flow. Accordingly, the problem is subdivided into two problems, one for the internal flow inside the enclosure and the other deals with the external flow. In the following, the method of analysis for each region is first presented and then the solution method for the coupled problem is explained.

3.1. The Internal Free Convection

The flow inside the enclosure is only driven by buoyancy forces and the equations governing the fluid motion are Equations (1-3). The boundary conditions are all defined in Equation (5) except for the temperature distribution [$\phi(x)$] on the top plate. To start the solution $\phi(x)$ will be first assumed and then corrected as will be explained in section 3.3. A variational finite-element method, similar to that developed by Badr [7-8] and Badr and Base [9], is used to solve Equations (1-3) inside the enclosure. In this method, the variational functional of each of Equations (1-3) is considered to be exactly the same as that of Poisson's equation. Accordingly, the non-linear terms in Equations (1) and (3) are considered invariant when obtaining the variational functional. These terms are approximated using the more recent values of the field variables (ψ, ζ, ϕ) in an iterative type solution. The functionals for these three equations can be written as:

$$I_\zeta = \int_A \left[\frac{1}{2} \left\{ \left(\frac{\partial \zeta}{\partial x} \right)^2 + \left(\frac{\partial \zeta}{\partial y} \right)^2 \right\} - \left\{ Ra \left(\frac{\partial \phi}{\partial x} \cos \theta - \frac{\partial \phi}{\partial y} \sin \theta \right) + \frac{1}{Pr} \left(\frac{\partial \psi}{\partial y} \frac{\partial \zeta}{\partial x} - \frac{\partial \psi}{\partial x} \frac{\partial \zeta}{\partial y} \right) \right\} \zeta \right] dA \quad (6)$$

$$I_\psi = \int_A \left[\frac{1}{2} \left\{ \left(\frac{\partial \psi}{\partial x} \right)^2 + \left(\frac{\partial \psi}{\partial y} \right)^2 \right\} - \zeta \psi \right] dA \quad (7)$$

$$I_\phi = \int_A \left[\frac{1}{2} \left\{ \left(\frac{\partial \phi}{\partial x} \right)^2 + \left(\frac{\partial \phi}{\partial y} \right)^2 \right\} + \left(\frac{\partial \psi}{\partial y} \frac{\partial \phi}{\partial x} - \frac{\partial \psi}{\partial x} \frac{\partial \phi}{\partial y} \right) \phi \right] dA \quad (8)$$

The extremization of each of these functionals with respect to the nodal values of the corresponding field variable results in a set of linear algebraic equations. The solution of the three sets of equations gives the distribution of the vorticity, stream function

and temperature all over the field. Details of the solution procedure are given in References [8–9] and need not to be repeated here.

3.2. The External Forced Convection

The top plate, which is considered to have a negligibly small thickness, is assumed to have infinite conductivity. The interaction between the internal and external heat transfer regimes leads to a non-uniform temperature distribution on that plate. According to the literature, there is no exact solution for the forced convective heat transfer from a flat plate having a non-uniform temperature distribution. The only approximate solution found is that by Kays [10] which provides the surface temperature on a flat plate with any arbitrary heat flux variation. This solution can be written in integral form as,

$$T(x) - T_\infty = \frac{0.623}{k} Pr^{-1/3} Re_x^{-1/2} \int_0^x \left[1 - \left(\frac{\xi}{x} \right)^{3/4} \right]^{-2/3} q_0(\xi) d\xi, \quad (9)$$

where $Re_x = Ux/\nu$ is the local Reynolds number at any station x , U is free stream velocity, ξ is the distance from the leading edge, and $q_0(\xi)$ is the heat flux variation.

In order to obtain the temperature distribution using Equation (9), the integral term must be evaluated, and this requires the heat flux distribution $q_0(\xi)$ to be known. After investigating several cases, the following second degree polynomial is found to approximate the heat flux with reasonable accuracy,

$$q_0(\xi) = a_0 + a_1\xi + a_2\xi^2. \quad (10)$$

The integral term was then calculated using the beta function and resulted in the following expression for the temperature distribution:

$$T(x) - T_\infty = \frac{0.623}{k} Pr^{-1/3} Re_x^{-1/2} \times \frac{4x}{3} (2.65a_0 + 2.02a_1x + 1.74a_2x^2). \quad (11)$$

3.3. The Coupling Between Internal and External Regimes

The thermal interaction between the internal and external heat transfer regimes occurs through the common conductive boundary (plate CD in Figure 1) which has an unknown temperature distribution $\phi(x)$.

This temperature distribution results from the heat balance between the two regimes. The mathematical solution of either one of the two problems requires prior knowledge of $\phi(x)$. In order to overcome this difficulty, only one of the two regions is considered at a time in a successive manner, the outcome of one being fed to the other across the common boundary, forming an iterative type solution method.

Initially, the stream function ψ and the vorticity ζ are assumed to be zero everywhere inside the enclosure. The temperature ϕ is also assumed zero everywhere except on the bottom plate (AB) where $\phi = 1$ (this may be similar to the situation when the bottom plate is suddenly heated in a time-dependent problem). The solution of the governing Equations (1–3) according to the method described in section 3.1 results in the new values for ψ , ζ , and ϕ inside the enclosure. The local heat flux distribution along the top plate (CD) is then calculated. This flux is now used in Equation (9) to obtain a better approximation for the temperature distribution on the plate. The obtained distribution $\phi(x)$ is again used as an improved boundary condition in the solution of the internal problem. The process continues until convergence is achieved.

4. DISCUSSION OF RESULTS

Before discussing results we first define the local and average heat transfer coefficients h and \bar{h} such that

$$h = \frac{k}{H} \left[\frac{\partial \phi}{\partial y} \right]_w, \quad \bar{h} = \frac{1}{L} \int_0^L h dx. \quad (12)$$

The local and average Nusselt numbers Nu and \bar{Nu} are defined as:

$$Nu = \frac{hH}{k} = - \left[\frac{\partial \phi}{\partial y} \right]_w, \quad \bar{Nu} = \frac{1}{L} \int_0^L Nu dx. \quad (13)$$

In order to verify the accuracy of the method of solution it was first used to solve the problem of natural convection inside a rectangular enclosure with two opposite isothermal walls. This problem has been studied extensively in the past. A comparison between the values of the average Nusselt number Nu obtained by previous investigators [11–15] and those obtained using the present method are shown in Table 1.

4.1. Local Heat Transfer Results

The variation of the local Nusselt number Nu along the cold plate (CD) for the two cases of

Table 1. Comparison Between \overline{Nu} Values Obtained from the Present Study and Those Obtained by Previous Investigators for the Standard Problem where $Ra = 1.47 \times 10^4$, $Pr = 0.733$, and $\theta = 90^\circ$.

Reference	\overline{Nu}
Tabarrok and Lin [11]	2.695
Reddy and Satake [12]	2.687
Catton <i>et al.</i> [13]	2.710
Wilkes <i>et al.</i> [14]	2.516
Ozoe <i>et al.</i> [15]	2.750
Present study	2.727

unidirectional and counter flows are shown in Figures 2a and 2b respectively. For unidirectional flow, Nu is highest at the leading edge ($x = 1$) and then decreases downstream. This is expected since the thermal boundary-layer thickness is zero at $x = 1$, giving rise to an infinite value of Nu as the trend shows in Figure 2a. The continuous decrease in Nu in the streamwise direction is also expected since the thermal boundary-layer thickens and the plate temperature decreases. For the counter flow regime, Nu decreases rapidly following the leading edge ($x = 0$) and reaching a minimum in the region $0 < x < 0.1$ as shown in Figure 2b. Following that point, Nu increases with x until reaching a maximum between $x = 0.1$ and $x = 1$. This increase in Nu is mainly due to the increase in the plate temperature. The location of Nu_{max} shifts downstream (towards $x = 1$) as AR increases as shown in the Figure. The counter flow nature of the internal and external flows tends to reduce the variation of Nu along the central portion of the top plate and gradually flattening it out with the increase of AR .

The variations of the local heat transfer along the hot plate (AB) for the two cases of unidirectional and counter flows are shown in Figure 3a and 3b respectively. In both cases, the value of Nu has its lowest at $x = 1$. This behavior is found to be independent of the angle of inclination, aspect ratio, or the Reynolds number of the external flow. The maximum heat transfer occurs near $x = 0$ in all cases since this is the region in which the descending cold fluid comes in contact with the hot plate. The point of Nu_{max} is found to move closer to $x = 0$ with the increase of AR . The streamlines for $AR = 1, 2$, and 4 are plotted in Figure 4a, b, and c respectively. The Figure shows that the high AR enclosure possesses higher velocities. Moreover, the descending cold

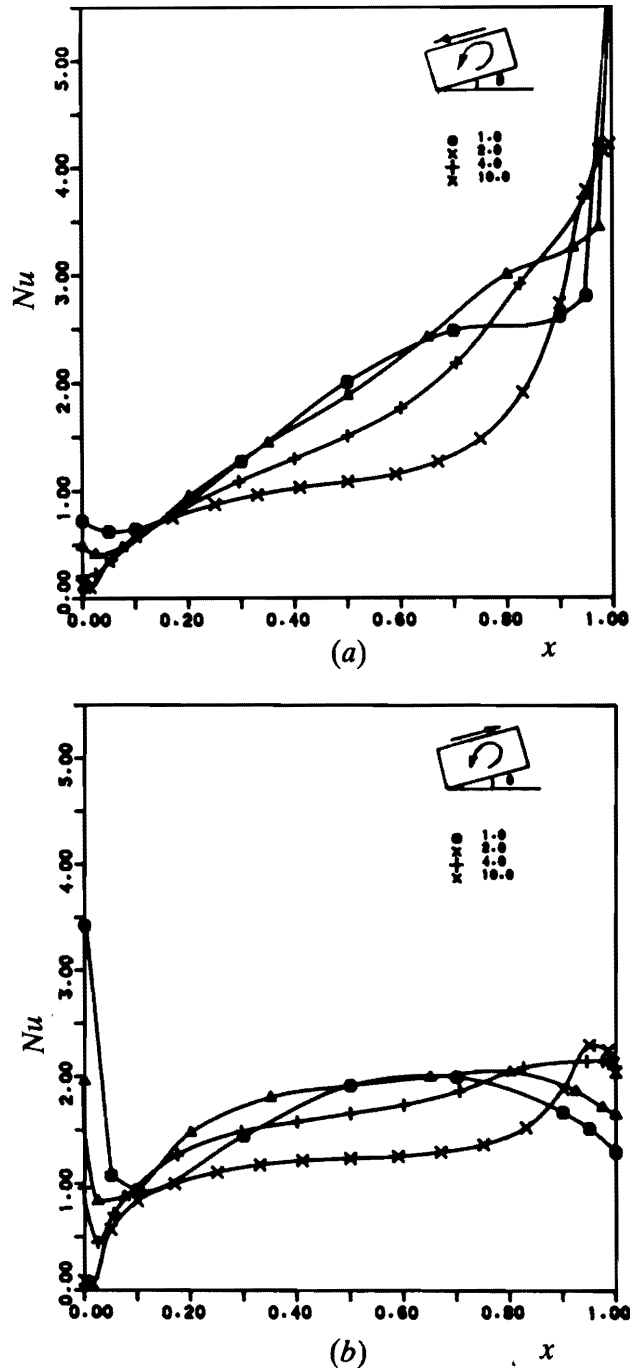
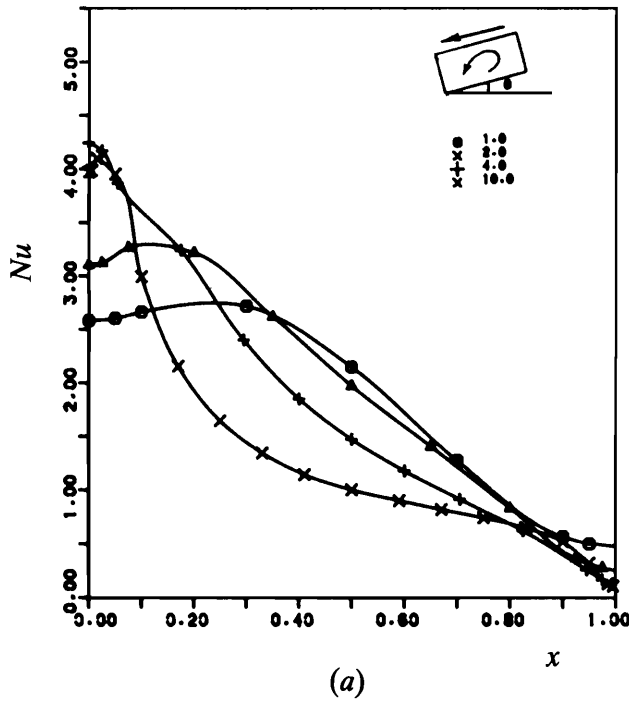
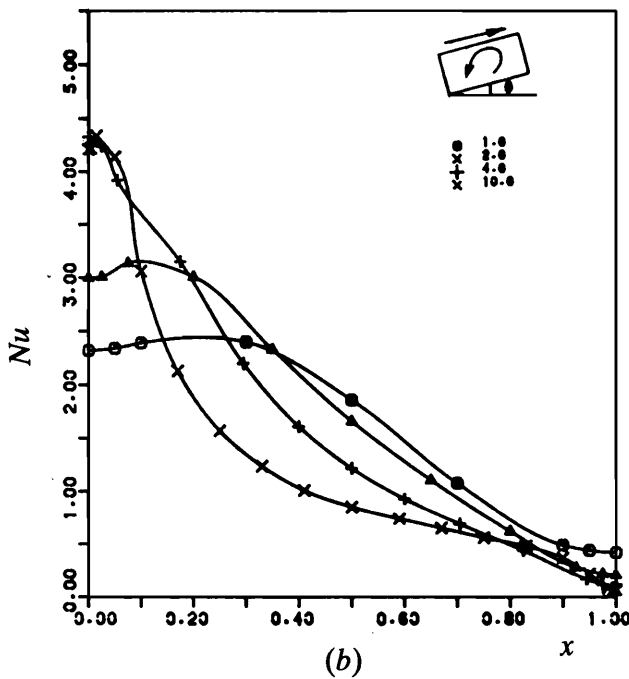


Figure 2. Variation of the Local Nusselt Number Along the Top Plate (CD).
(a) unidirectional flow and (b) counter flow.

fluid comes in contact with the hot plate closer to the corner at A. This matches well with the location of Nu_{max} explained above and shown in Figure 3. The effect of the external flow direction on the Nu distribution along the hot plate is shown in Figure 5a and b for the cases of $AR = 1$, and 10, respectively. The



(a)



(b)

Figure 3. Variation of the Local Nusselt Number Along the Hot Plate (AB).
(a) unidirectional flow and (b) counter flow.

Figure shows that the values of Nu for unidirectional flow are slightly lower than those for the counter flow, otherwise the trends are similar.

4.2. Average Heat Transfer Results

The effect of the aspect ratio on the average Nusselt number is shown in Figures 6 and 7 for the cases of unidirectional and counter flows. The Figures show that enclosures with $AR = 2$ provide the maximum heat transfer for all ranges of parameters considered for both flow regimes. Similar findings have been reported for the noncoupled problem by Randall *et al.* [16] and also by Schinkel *et al.* [17]. Increasing AR above 2 tends to decrease the average Nusselt number.

The effect of the angle of inclination θ on the heat transfer is shown in Figure 8 for unidirectional flow and in Figure 9 for counter flow. Figure 8 shows that \bar{Nu} reaches a maximum at $\theta = 80^\circ$ for $AR = 10$, however, for $AR = 2$ the maximum \bar{Nu} occurs at a much lower angle. The trend for the case of counter flow is similar (see Figure 9), but the maximum \bar{Nu} for the highest aspect ratio considered ($AR = 10$) occurs at $\theta = 90^\circ$ while occurring at $\theta = 40^\circ$ for the lowest aspect ratio ($AR = 1$). In general, it is found that for $AR < 4$ the maximum \bar{Nu} occurs between $\theta = 40^\circ$ and $\theta = 60^\circ$, however, as AR increases above 4 the angle θ producing maximum \bar{Nu} was found to shift towards the vertical. The values of \bar{Nu} for unidirectional flow are found to be 5–8% less than those for the counter flow but the maximums in both cases occur approximately at the same angles of inclination. The effect of the inclination angle on the velocity field inside the enclosure can be seen in Figure 10a and b which shows the variation of u with y at $x = 0.5$. For low aspect ratios, it is found that increasing θ results in decreasing the velocity in the enclosure which tends to decrease the rate of heat transfer as shown in Figure 10a. The opposite occurs for high AR enclosures as shown in Figure 10b. This explains the phenomenon presented above. Maximum heat transfer was also found to occur between $\theta = 0^\circ$ and $\theta = 90^\circ$ for the standard problem by Ozoe *et al.* [18], Writz and Tseng [19], and Arnold *et al.* [20].

4.3. The Temperature Variations

The temperature variations on the top plate for the case of unidirectional flow are shown in Figure 11a and b for the two aspect ratios of 1 and 10 and for the two inclination angles and two Reynolds numbers in each case. The Figure shows that the temperature increases from zero at the leading edge ($x = 1$) to a maximum at $0.6 < x < 0.8$ and then

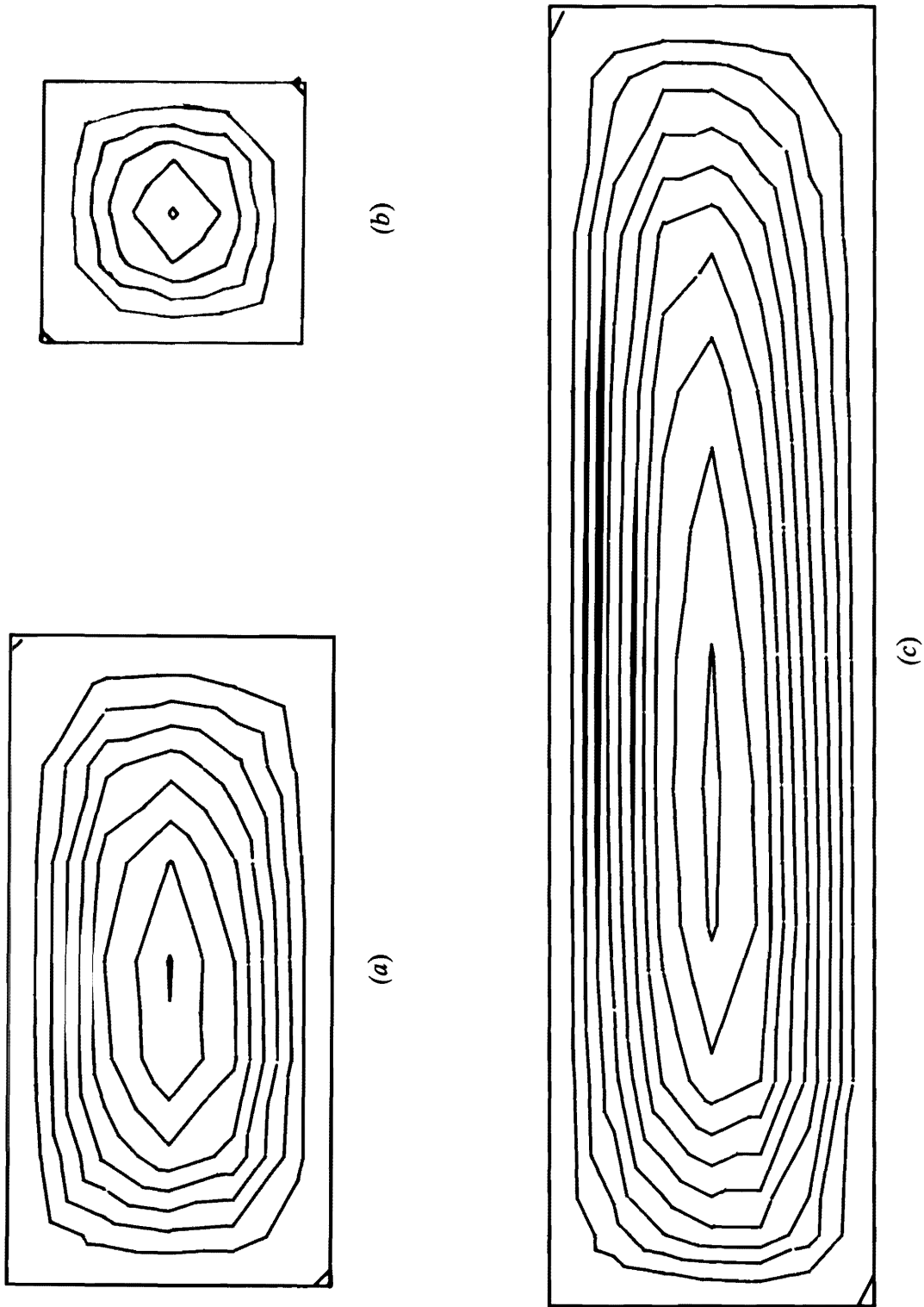


Figure 4. The Streamline Pattern Inside the Enclosure for the Case of $Re = 8 \times 10^3$, $Re = 3 \times 10^5$, and $\theta = 60^\circ$.
(a) $AR = 1$, (b) $AR = 2$, (c) $AR = 4$. (The streamlines plotted are $\psi = 0, 1, 2, 3, 4, \dots$.)

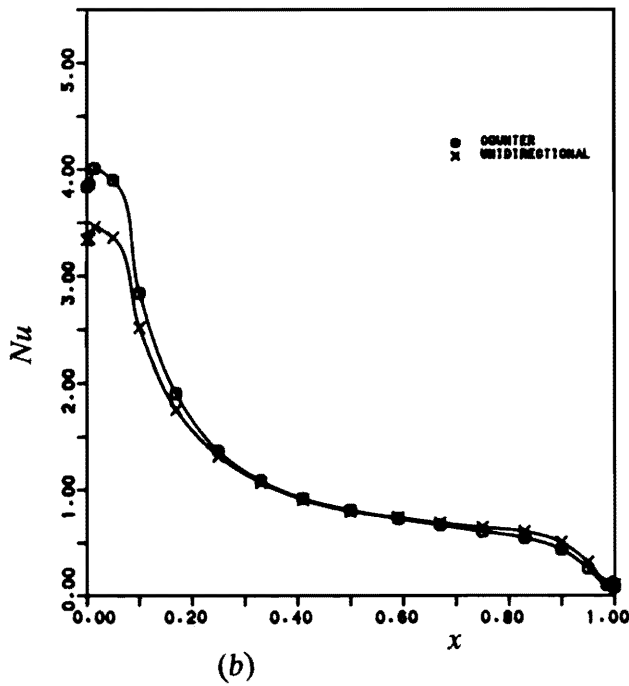
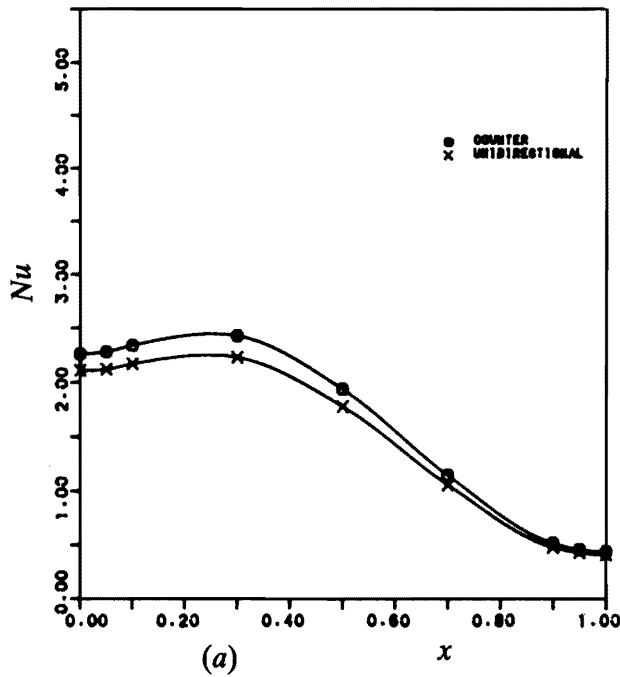


Figure 5. Effect of External Flow Direction on the Local Nusselt Number Variation Along the Hot Plate (AB).
(a) $AR = 1$, (b) $AR = 10$.

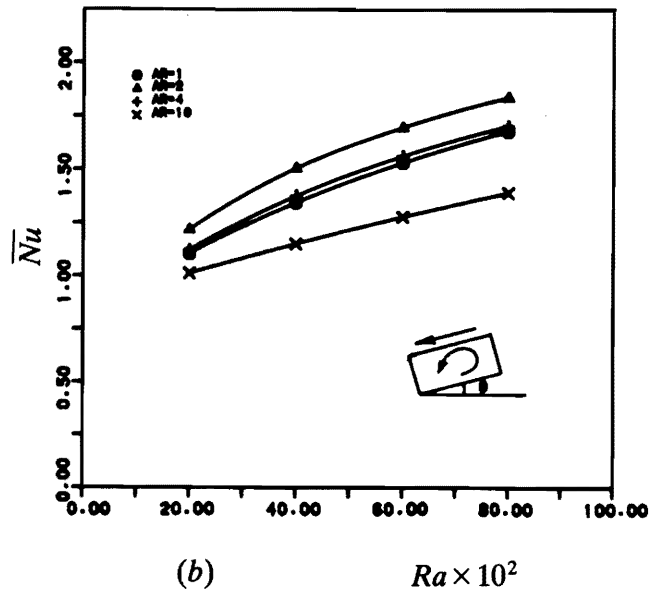
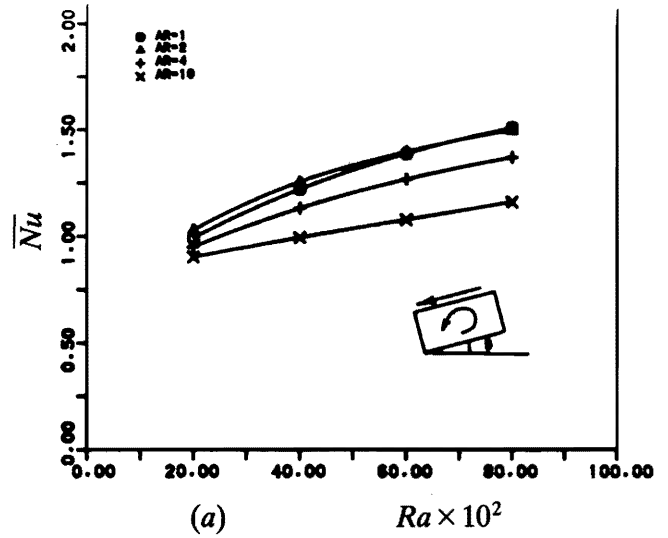


Figure 6. Effect of Rayleigh Number on the Average Nusselt Number for the Case of Unidirectional Flow.
(a) $Re = 6 \times 10^4$ and $\theta = 60^\circ$, (b) $Re = 3 \times 10^5$ and $\theta = 90^\circ$.

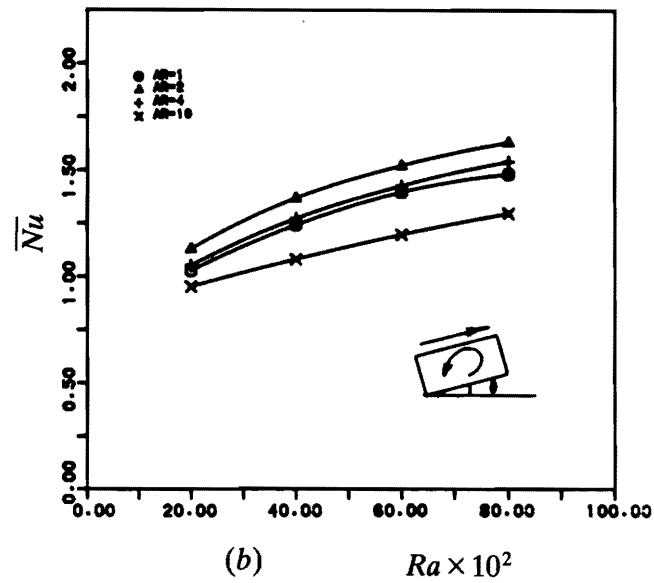
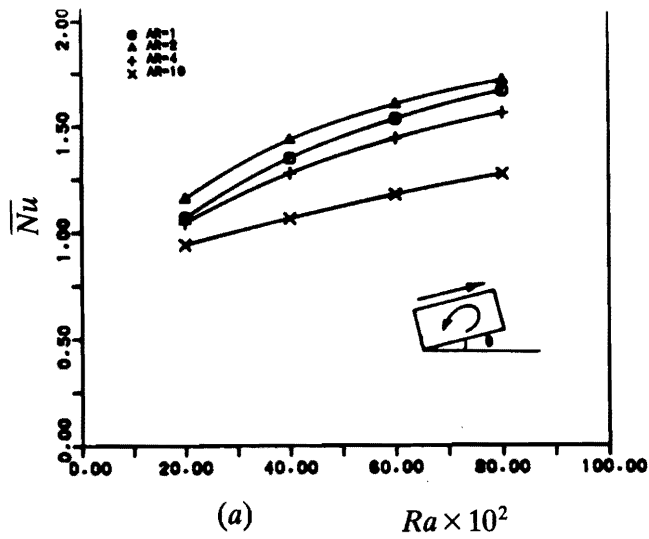


Figure 7. Effect of Rayleigh Number on the Average Nusselt Number for the Case of Counter Flow. (a) $Re = 6 \times 10^4$ and $\theta = 60^\circ$, (b) $Re = 6 \times 10^4$ and $\theta = 90^\circ$.

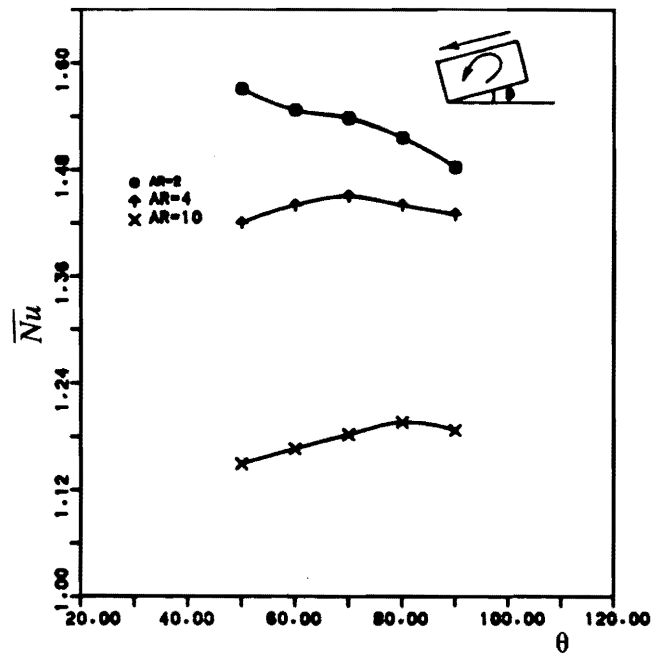


Figure 8. Variation of the Average Nusselt Number with the Inclination Angle for the Case of Unidirectional Flow when $Ra = 8 \times 10^3$ and $Re = 6 \times 10^4$.

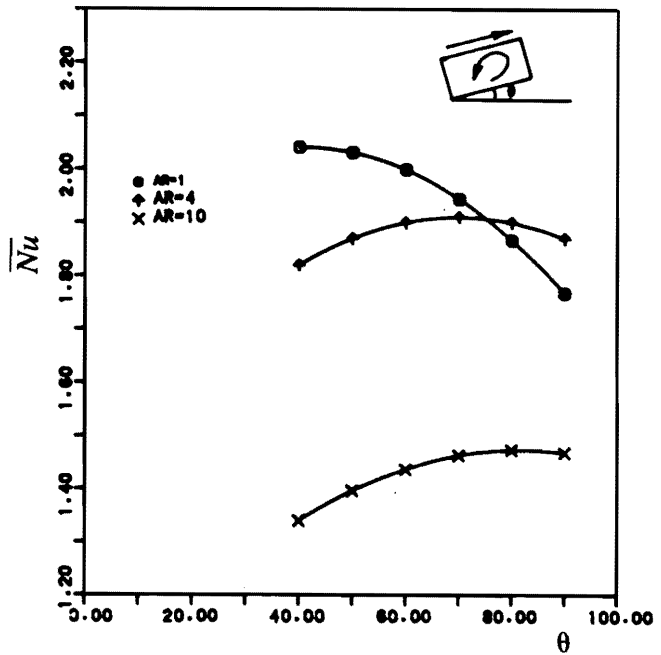


Figure 9. Variation of the Average Nusselt Number with the Inclination Angle for the Case of Counter Flow when $Ra = 8 \times 10^3$ and $Re = 3 \times 10^5$.

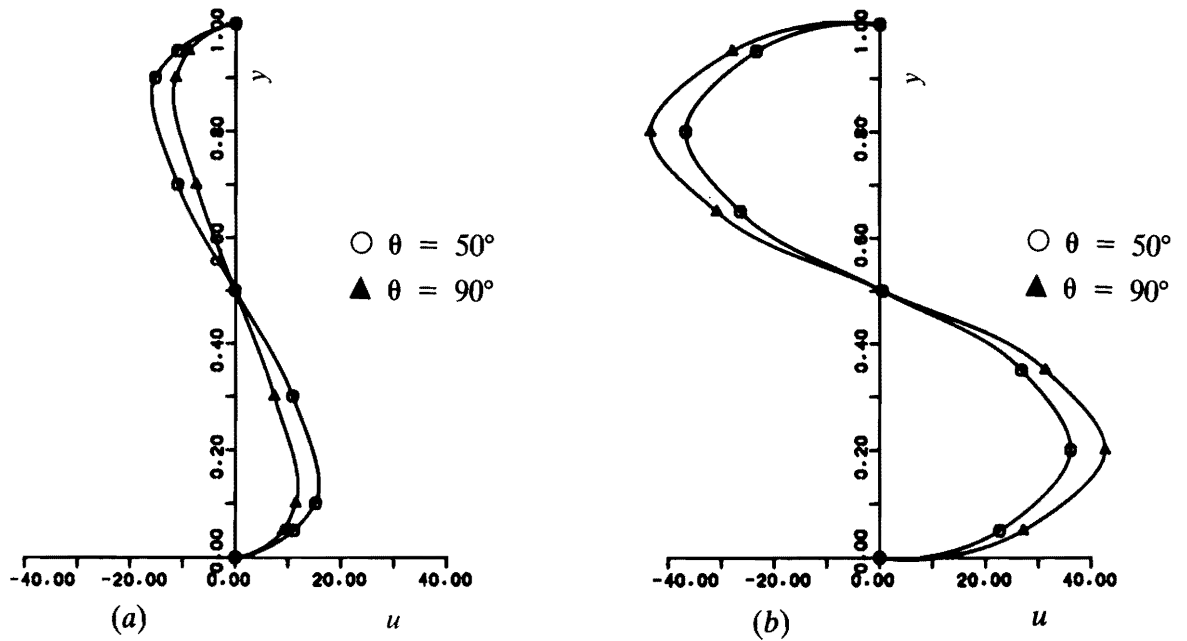


Figure 10. The Effect of Angle of Inclination on the Velocity Distribution at Section $x = 0.5$ for the Case of Counter Flow when $Ra = 8 \times 10^3$ and $Re = 3 \times 10^5$. (a) $AR = 1$; (b) $AR = 10$.

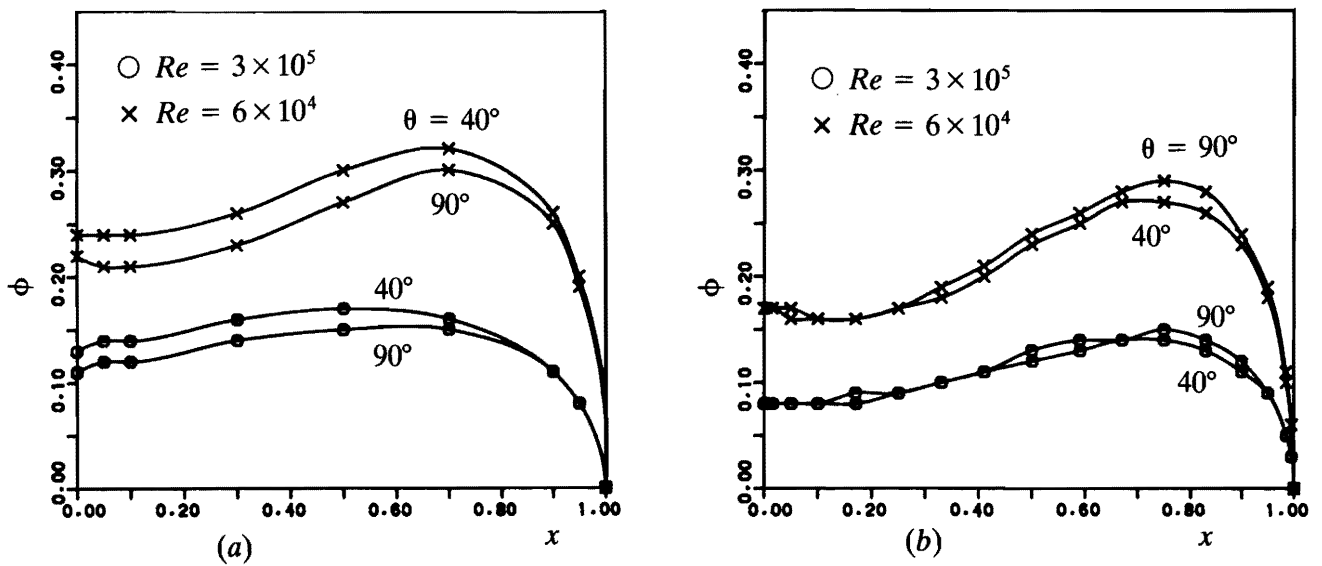


Figure 11. The Temperature Variation on the Top Plate (CD) for the Case of Unidirectional Flow when $Ra = 8 \times 10^3$. (a) $AR = 1$; (b) $AR = 10$.

levels off to an intermediate value. The effect of increasing Re of the external flow is to decrease the temperature everywhere on the plate. On the other hand, the increase of the inclination angle tends to decrease the temperature on the top plate for low aspect ratio enclosures while increasing it for the high aspect ratio ones. This effect causes the average Nusselt number \overline{Nu} to increase with the increase of θ for high AR enclosures while the opposite occurs for low AR ones.

The temperature variations on the top plate for the case of counter flow are shown in Figure 12a and b for the same parameters as in Figure 11. The Figure shows that ϕ increases on the top plate continuously starting from the leading edge ($x = 0$). The effect of the inclination angle on the temperature distribution is similar to that found in the case of unidirectional flow. The reason for this is the change in the velocities inside the enclosure as shown in Figure 10.

The phenomenon of temperature reversal which has been reported in References [2, 4] is found to occur in this study when $Ra > 8 \times 10^3$ for enclosures of different aspect ratios and angles of inclination. The isotherms showing this phenomenon for the case of counter flow are given in Figure 13 for $AR = 1, 2,$ and 4 . It is found that increasing Re of external flow affects only slightly the temperature reversals. For the range of parameters considered in this study, no temperature reversal occurred in the case of unidirectional flow.

All computations were carried out using AMDAHL 580 computer. The CPU time ranged from 20 seconds for aspect ratio $AR = 1$ to about 200 seconds for $AR = 10$. The number of iterations required for convergence ranged from 250 to a maximum of 850.

5. CONCLUSIONS

The study showed that the effect of coupling between the internal natural convection and external forced convection is a reduction of the average heat transfer below that of the standard problem. The heat transfer is found to increase with the increase of the external flow Reynolds number. The aspect ratio of 2 resulted in maximum heat transfer for all cases considered. For $AR < 4$ the average heat transfer decreases with increasing the angle of inclination while the opposite occurs for $AR > 4$. Temperature reversals occur inside the enclosure when $Ra > 8 \times 10^3$ for

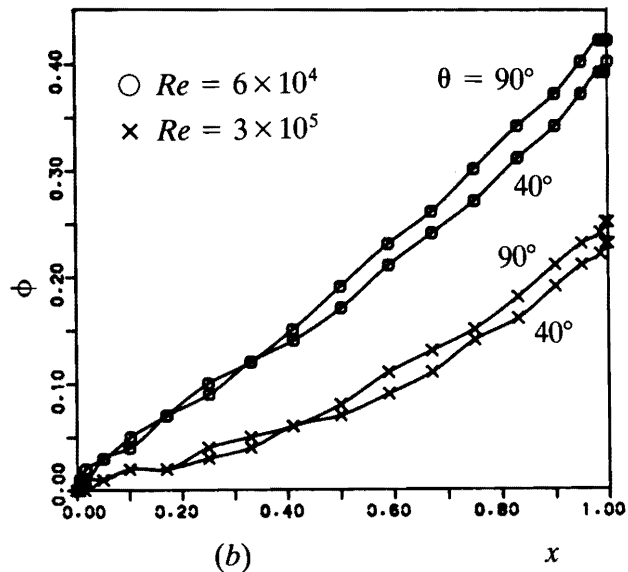
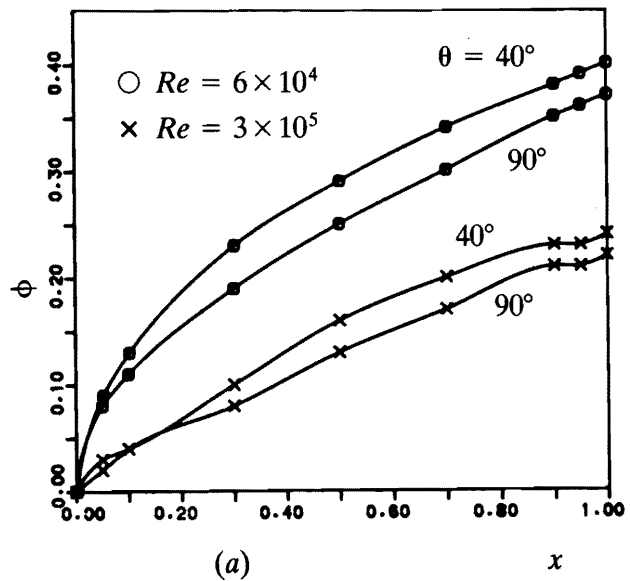


Figure 12. The Temperature Variation on the Top Plate (CD) for the Case of Counter Flow when $Ra = 8 \times 10^3$. (a) $AR = 1$; (b) $AR = 10$.

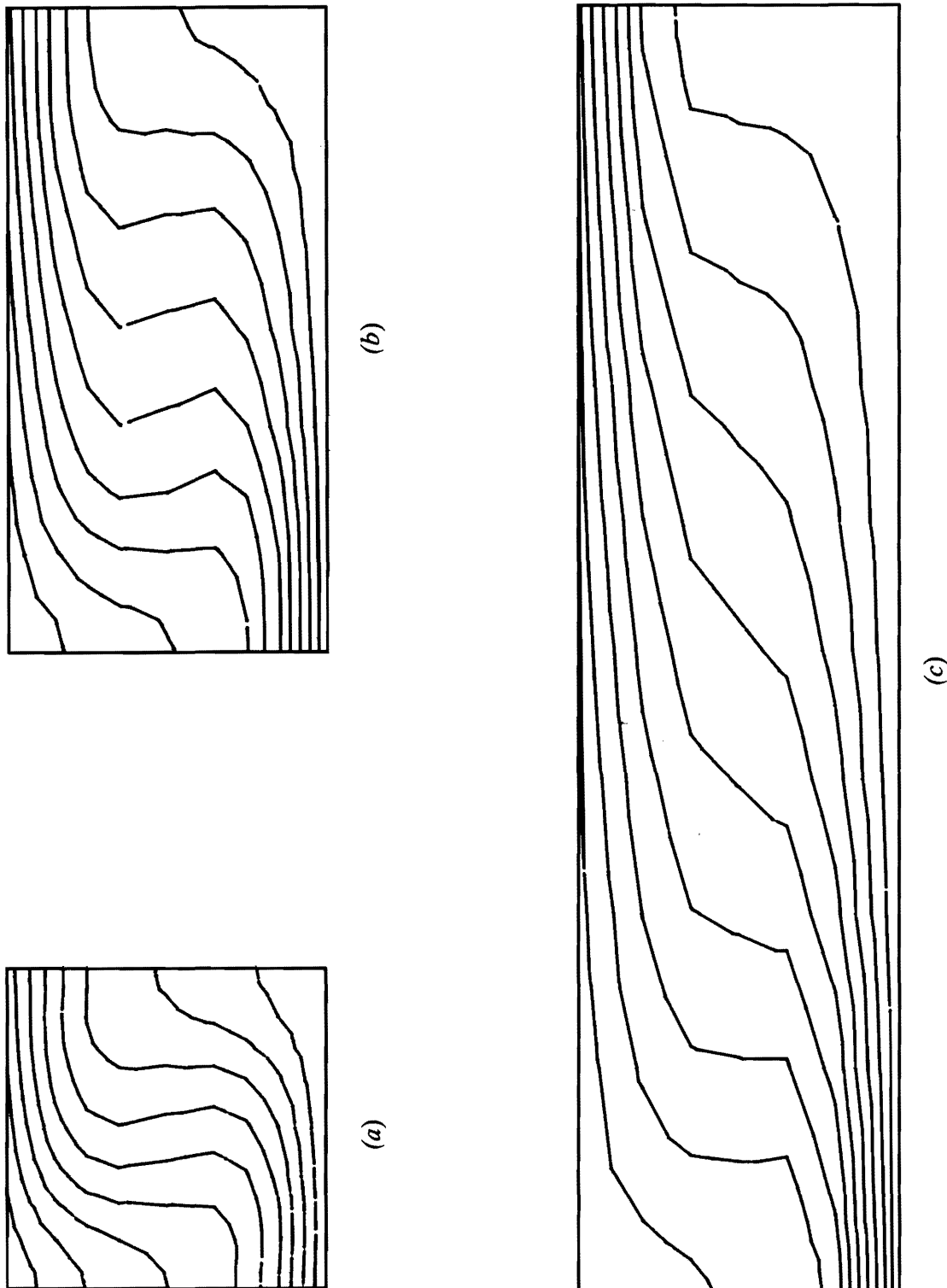


Figure 13. The Isotherm Pattern Inside the Enclosure for the Case of Counter Flow when $Ra = 8 \times 10^3$, $Re = 3 \times 10^5$, and $\theta = 60^\circ$. (a) $AR = 1$; (b) $AR = 2$; (c) $AR = 4$. (The isotherms plotted are $\phi = 0.0, 0.1, 0.2, 0.3, \dots, 0.9$.)

the counter flow regime. However, no temperature reversals occur for the unidirectional flow case in the considered range of various parameters. The counter flow regime results in heat transfer rates about 5–8% higher than those for unidirectional flow.

ACKNOWLEDGEMENTS

The authors wish to acknowledge the support received from King Fahd University of Petroleum & Minerals during the course of this study.

REFERENCES

- [1] I. Catton, "Natural Convection in Enclosures", *Proceedings of the Sixth International Heat Transfer Conference, Toronto, Canada, August 1978*, vol. 6, p. 13.
- [2] T. G. Karayiannis, "An Interferometric Study of the Coupled and Non-Coupled Convective Heat Transfer from an Inclined Rectangular Cavity", *Ph.D. Thesis, University of Western Ontario, London, Ontario, 1985*.
- [3] E. M. Sparrow and Prakash, "Interaction Between Internal Natural Convection in an Enclosure and an External Natural Convection Boundary-Layer Flow", *International Journal of Heat and Mass Transfer*, **24** (1981), p. 895.
- [4] N. N. Saidi, "An Interferometric Study of Coupled Convective Heat Transfer in a Horizontal Flat Plate Enclosure", *Ph.D. Thesis, University of Western Ontario, London, Ontario, 1983*.
- [5] N. N. Saidi, J. D. Tarasuk, and T. E. Base, "The Coupling Effect Between Natural Heat Convection Inside the Cavity of a Solar Collector and External Forced Convection Heat Transfer", *Energex 82, Canada's International Energy Exposition and Conference, Regina, 1982*.
- [6] T. G. Karayiannis and J. D. Tarasuk, "Influence of Temperature Characteristics of the Upper Surface on the Heat Transfer in a Solar Collector", *Transactions of the Canadian Society for Mechanical Engineering*, **9** (1985), p. 32.
- [7] H. M. Badr, "Response of the Laminar Layer on a Flat Plate to Free Stream Disturbances", *Ph.D. Thesis, University of Western Ontario, London, Ontario, 1977*.
- [8] H. M. Badr, "Study of Laminar Free Convection Between Two Eccentric Horizontal Tubes", *Transactions of the Canadian Society for Mechanical Engineering*, **7** (1983), p. 191.
- [9] H. M. Badr and T. E. Base, "A Variational Finite Element Method for Solving Unsteady Viscous Flow Problems", *Transactions of the Canadian Society for Mechanical Engineering*, **5** (1978), p. 39.
- [10] W. M. Kays, *Convective Heat and Mass Transfer*. New York: McGraw-Hill, 1966.
- [11] B. Tabarrok and R. C. Lin, "Finite Element Analysis of Free Convection Flows", *International Journal of Heat and Mass Transfer*, **20** (1977), p. 945.
- [12] J. N. Reddy and A. Satake, "A Comparison of Penalty Finite Element Model with the Stream Function-Vorticity Model of Natural Convection in Enclosures", *ASME Journal of Heat Transfer*, **102** (1980), p. 659.
- [13] I. Catton, P. S. Ayyaswami, and R. C. Clever, "Natural Convection Flow in a Rectangular Slot Arbitrarily Oriented with Respect to the Gravity Vector", *International Journal of Heat and Mass Transfer*, **17** (1974), p. 173.
- [14] J. O. Wilkes and S. W. Churchill, "The Finite Difference Computation of Natural Convection in a Rectangular Enclosure", *AIChE Journal*, **12** (1966), p. 161.
- [15] H. Ozoe, H. Sayama, and S. W. Churchill, "Natural Convection in an Inclined Rectangular Channel at Various Aspect Ratios and Angles—Experimental Measurements", *International Journal of Heat and Mass Transfer*, **18** (1975), p. 1425.
- [16] K. R. Randall, J. W. Mitchell, and M. M. El-Wakil, "Natural Convection Heat Transfer Characteristics of Flat Plate Enclosures", *Journal of Heat Transfer*, **101** (1979), p. 120.
- [17] W. M. Schinkel and C. J. Hoogendoorn, "An Interferometric Study of the Local Heat Transfer by Natural Convection in Inclined Air Filled Enclosures", *Proceedings of the Sixth International Heat Transfer Conference*, **6** (1978), p. 281.
- [18] H. Ozoe, K. Yamamoto, H. Sayama, and S. W. Churchill, "Natural Circulation in an Inclined Rectangular Channel Heated on One Side and Cooled on the Opposite Side", *International Journal of Heat and Mass Transfer*, **17** (1974), p. 1209.
- [19] R. A. Wirtz and W. F. Tseng, "Natural Convection Across Tilted Rectangular Enclosure of Small Aspect Ratios", *Proceedings of the 19th National Heat Transfer Conference, Orlando, Florida, 1980*, p. 47.
- [20] J. N. Arnold, I. Catton, and D. K. Edwards, "Experimental Investigation of Natural Convection in Inclined Rectangular Regions of Differing Aspect Ratios", *ASME Journal of Heat Transfer*, **98** (1976), p. 67.

Paper Received 30 April 1988; Revised 9 October 1989.